Recibido: 29/06/2015
Aceptado: 14/03/2016

REVISTA DE TELEDETECCIÓN
Asociación Española de Teledetección
(2016) 46, 103-117
ISSN 1133-0953
EISSN 1988-8740
http://dx.doi.org/10.4995/raet.2016.3980

Cartografía de variables dasométricas en bosques Mediterráneos mediante análisis de los umbrales de altura e inventario a nivel de masa con datos LiDAR de baja resolución

Guerra-Hernández, J.[1], Tomé, M.[1], González-Ferreiro, E.[2,3,4]

[1] *Centro de Estudos Florestais (CEF), Universidade de Lisboa, Instituto Superior de Agronomía, Tapada da Ajuda, P 1349-017 Lisboa, Portugal.*

[2] *Unidade de Xestión Forestal Sostible (GI-1837-UXFS). Departamento de Enxeñería Agroforestal, Universidade de Santiago de Compostela, Escola Politécnica Superior, R/ Benigno Ledo, Campus Universitario, E 27002 Lugo, Spain.*

[3] *Department of Forest Ecosystems and Society (FES), Oregon State University, 321 Richardson Hall, Corvallis, OR 97331, USA.*

[4] *Laboratory of Applications of Remote Sensing in Ecology (LARSE), US Forest Service - Pacific Northwest Research Station, 3200 SW Jefferson Way, Corvallis, OR 97331, USA.*

Resumen: Este estudio presenta avances en la metodología de inventario forestal a nivel de masa (*area-based approach, ABA*) con datos LiDAR aerotransportado de baja densidad y destaca la utilidad de los datos LiDAR disponibles para España a escala nacional para realizar cartografía de las principales variables dasométricas en un bosque Mediterráneo de pino piñonero, caracterizado por una compleja orografía. Para ello, se ajustaron modelos lineales de regresión en cada tipo de bosque, a partir de los datos LiDAR de baja densidad (0,5 primeros retornos m^{-2}), proporcionados por el PNOA (Plan Nacional de Ortofotografía Aérea) y los datos obtenidos en campo. Además, se investigó la influencia de los umbrales de altura usados en la extracción de los estadísticos de la nube de puntos LiDAR (*MHT: Minimun Height Threshold* y *BHT: Break Height Threshold*). Los mejores modelos de regresión explicaron un 61-85%, 67-98%, 74-98% de la variabilidad en altura de masa, área basimétrica y volumen, respectivamente. El error de estimación en las variables de masa fue mayor en bosques cerrados mixtos y puros de caducifolias que en los bosques más homogéneos de coníferas. Los resultados demostraron que los umbrales de altura no fueron especialmente críticos en la estimación de las variables de masa en bosques de coníferas, pero hubo diferencias sustanciales en el caso de volumen, cuando aumentaron los umbrales de altura (*HBT* y *MHT*) en las masas de estructura más compleja (bosque mixto y puro de caducifolias). Un análisis métrica a métrica reveló la existencia de diferencias significativas en la mayor parte de las variables explicativas extraídas a partir de diferentes umbrales de altura (*HBT* y *MHT*). Los mejores modelos de predicción se aplicaron a los rodales de referencia y se elaboró una cartografía espacialmente explícita que representa las principales variables de masa, facilitando así la toma de decisiones para la gestión forestal sostenible en los ecosistemas de bosque mediterráneo.

Palabras clave: Láser escáner aerotransportado, inventario forestal, cartografía atributos forestales, teledetección, modelización forestal.

Using low density LiDAR data to map Mediterranean forest characteristics by means of an area-based approach and height threshold analysis

Abstract: This study reports progress in forest inventory methods involving the use of low density airborne LiDAR data and an area-based approach (ABA). It also emphasizes the usefulness of the Spanish countrywide LiDAR dataset

* *Autor para la correspondencia: juanguerra@isa.ulisboa.pt*

for mapping forest stand attributes in Mediterranean stone pine forest characterized by complex orography. Low-density airborne LiDAR data (0.5 first returns m^{-2}) was used to develop individual regression models for a set of forest stand variables in different types of forest. LiDAR data is now freely available for most of the Spanish territory and is provided by the Spanish National Aerial Photography Program (*Plan Nacional de Ortofotografía Aérea, PNOA*). The influence of height thresholds (*MHT: Minimun Height Threshold* and *BHT: Break Height Threshold*) used in extracting LiDAR metrics was also investigated. The best regression models explained 61-85%, 67-98% and 74-98% of the variability in ground-truth stand height, basal area and volume, respectively. The magnitude of error for predicting structural vegetation parameters was higher in closed deciduous and mixed forest than in the more homogeneous coniferous stands. Analysis of height thresholds (*HT*) revealed that these parameters were not particularly important for estimating several forest attributes in the coniferous forest; nevertheless, substantial differences in volume modelling were observed when the height thresholds (*MHT* and *BHT*) were increased in complex structural vegetation (mixed and deciduous forest). A metric-by-metric analysis revealed that there were significant differences in most of the explanatory variables computed from different height thresholds (*HBT* and *MHT*).The best models were applied to the reference stands to yield spatially explicit predictions about the forest resources. Reliable mapping of biometric variables was implemented to facilitate effective and sustainable management strategies and practices in Mediterranean Forest ecosystems.

Key words: Airborne laser scanning data, forest inventory, forest attribute mapping, remote sensing, forest modelling.

1. Introduction

Analysis of the spatial distribution of biomass and forest inventory parameters is required in order to support forest management decisions in Mediterranean Forest ecosystems. Optical remotely sensed data is often used for such purposes; however, it is often difficult to estimate the parameters in areas characterized by a complex forest structure. During the past three decades, airborne LiDAR has become an established method for accurate derivation of the most important forest inventory parameters (Maltamo *et al.,* 2014).

Single-tree and stand-level approaches can be used with LiDAR data to estimate forest parameters. In the former approach, single-tree attributes are estimated by crown delineation, height measurement and detection of individual apexes. However, the performance of this approach is relatively poor in complex stands where individual tree segmentation algorithms frequently generate commission/omission errors during analysis of individual trees (González-Ferreiro *et al.,* 2013). This approach is also very expensive as it requires spatially dense LiDAR data. The area-based approach (ABA) is a less expensive alternative and has commonly been used to generate maps of forest attributes over a wide range of forest types: Temperate (Hall *et al.,* 2005), Boreal (Næsset and Gobakken 2008), Atlantic (Gonçalves-Seco *et al.,* 2011; González-Ferreiro *et al.,* 2012) and Mediterranean forests (González-Olabarria *et al.,* 2012; Alberti *et al.,* 2013). This approach establishes statistical relationships between plot-level LiDAR metrics and stand attributes such as stand height, basal area and volume, which are derived from field measurements.

Some studies have investigated the influence of two height thresholds (*HT*) used during extraction of LiDAR metrics (Næsset, 2011; Nyström *et al.,* 2012; Görgens, 2015): *i*) the minimum height threshold (*MHT*), which is commonly specified as the lower boundary for calculating height metrics, and *ii*) the height break threshold (*HBT)*, which is the limit for separating the point cloud data into two sets, as when the canopy returns are separated from the under canopy group. The *MHT* and *HBT* can be established independently and a wide range of values can be applied, especially for mature forests where most returns are obtained from biological material located some distance above the ground (Næsset 2011). However, in young, closed deciduous and mixed forest, selection of a more specific threshold value will probably have a greater impact on estimation of the forest stand attributes.

The *MHT* can be obtained by various approaches. The first approach selects a threshold value that splits the cloud into below-canopy and canopy returns; a value of 2 m is often used for splitting the canopy (e.g. Næsset, 2002; Næsset, 2011; Montaghi *et al.,* 2013). A second approach uses the *MHT* to exclude returns not considered as necessary for estimating certain variables; thus,

for example, returns below the lowest average height of the smallest trees measured are usually removed for volume estimation (e.g. Jensen *et al.,* 2006; Montagnoli *et al.,* 2015). The third approach deals with noise from ground classification errors and aims to eliminate returns from understory, stones, dead wood and other non-relevant elements (e.g. García *et al.,* 2010). For the *HBT*, the cloud is split into two sets to calculate proportions (canopy density metrics or metrics related to crown closure). The threshold can be established on the basis of canopy base height (e.g. Andersen *et al.,* 2005) or it can be defined as a function of other metrics for the whole study area, e.g. mean, mode or percentiles (Næsset, 2002). A *HT* analysis is important to separate the returns from canopy and below canopy, remove unnecessary returns or noise, and hence in forest variables modelling, since LiDAR metrics should describe biophysical characteristics of the analysed stands.

In this study, we used the ABA to derive forest information from low-density countrywide LiDAR data in a Mediterranean forest in southwestern Spain. The overall objectives of the study were as follows: *i*) to use LiDAR data to develop predictive linear models of biometric parameters for 4 different types of forest; *ii*) to investigate the effects of height thresholds (*MHT* and *HBT*) on the explanatory capacity of a set of metrics aimed at estimating stand variables in the different types of forest; and *iii*) to use the LiDAR-derived models to map the stand variables across the landscape.

2. Material and methods

2.1. Study area

This study was conducted in the public *Tudia y sus Faldas* forest located near the town of Monasterio (Region of Extremadura, SW Spain) (Figure 1) (Guerra-Hernández *et al.,* 2015). The forest area, corresponding to public utility forest number 1 (*MUP1*, *Monte de Utilidad Pública número 1*), covers an area of 748.20 ha. The forest is representative of stone pine forest in SW Spain, characterized by the dominance

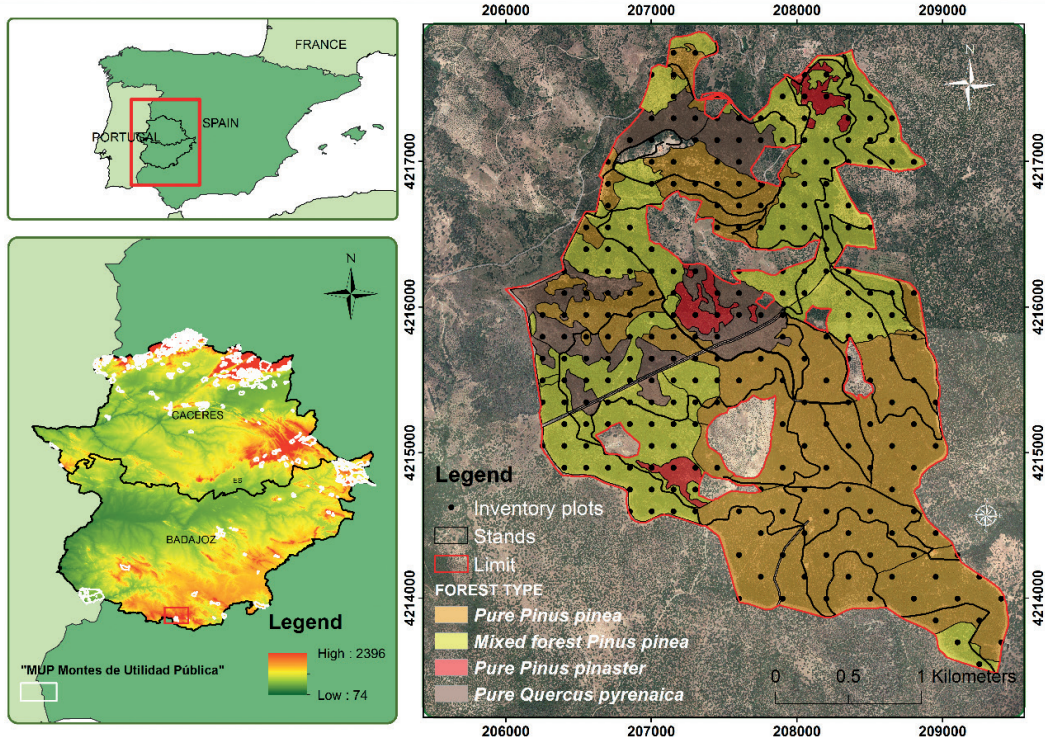

Figure 1. Boundary of the *Tudia y sus Faldas* forest study site (red line), forest types (coloured polygons), and forest inventory plots (black dots).

of pure stone pine (*Pinus pinea* L.) stands and mixed forest of stone pine stands associated with maritime pine (*Pinus pinaster* Ait.) and Pyrenean oak (*Quercus pyrenaica* Willd.). The MUP1 also includes a small proportion of pure Pyrenean oak and maritime pine stands. The elevation of the study area ranges from 600 to 1100 m.a.s.l., and the average slope is 25.5%.

2.2. Plot data

Field data were obtained from the forest inventory carried out by the Extremadura Forest Service for forest management purposes. According to forestry management regulations in Spain, for a random stratified inventory, a maximum sampling error of 15% in the basal areal is allowed with a fiducial probability of 95%. On the basis of this condition, the theoretical number of plots for each stratum was calculated according to an optimal and proportional allocation (systematically distributed in a grid of approximately 200×200 m for pure stands of stone pine and 150×150 m for the other strata). In total, 192 circular sample plots of 11 m radius (area of 380.13 m^2) were measured in the study area, between July and August 2010. From these reference points, a LEICA GX1230 (dual frequency real time kinematic receiver with a planimetric precision of ±5 mm+0.5 ppm and an altimetric precision of ±10 mm+0.5 ppm) was used, along with a metal detector, to relocate the centre of each plot (marked with iron poles). At each point, GPS signals were logged using a roving receiver with an external antenna (ATX1230 GG), and the recordings were post-processed with correction data retrieved from the fixed base station in Llerena (Badajoz) (station number: 355919, X: 236491.04585 m, Y: 4236374.10125 m, Coordinates system ETRS89-30, and Altitude: 642.39223 m), to give the plot positions. All trees of dbh (diameter at breast height) >7.5 cm were measured in each plot. Small trees (dbh <7.5 cm) were also tallied for the total stem number, but the data were not used in basal area and volume calculations. The tree height, height to crown base, crown width (in two directions at right angles to each other) and age were measured in a subsample of 3 trees per plot (the northernmost, southernmost and one dominant tree). The heights of the remaining trees were estimated by using locally adjusted allometric models. The following equations were used to estimate the height of all trees in the sample plots (Table 1):

Table 1. Non-linear height-diameter models.

Specie	Equation	RMSE
P. pinea (*n*=361)	$h = 0.0633024 \cdot d^{0.862396}$	1.313
P. pinaster (*n*=68)	$h = 1.3 + \frac{d^2}{(19.6814 + 0.22983 \cdot d)^2}$	2.26
Q. pyrenaica (*n*=103)	$h = 1.3 + \frac{d^2}{(33.0519 + 0.170836 \cdot d)^2}$	1.303

where h is total tree height (m), d is diameter at breast height (1.3 m above the ground level, mm).

Stand height (*SH*) was computed as Lorey's mean height (defined as a basal-area-weighted average height), which is the definition of stand height that provides the values closest to the aerodynamic canopy height in pine forest stands (Nakai *et al.,* 2010) and is expected to adequately represent the average height of the dominant and co-dominant trees in a stand (González-Ferreiro *et al.,* 2014). The volume over bark of each tree was estimated using the non-linear models developed by the Spanish National Forest Inventory for *P. pinea, P. pinaster* and *Q. pyrenaica* in Badajoz (Extremadura). The field measurements (diameters, heights and heights to crown base) were used to estimate the following stand variables in each plot, on a per hectare basis: mean height (H_m), stand height (*SH*), dominant height (H_0), stand basal area (*G*), stand volume over bark (*V*), canopy base height (*CBH*) (Table 2).

Further analysis was performed considering four types of forest: *i*) pure *P. pinea*, *ii*) mixed, *iii*) *Q. pyrenaica* forest, and *iv*) *P. pinaster*. The forest type was considered dominant if the basal area of the dominant species represented more than 70% of *G* within the plot. Following this criterion, 120 plots were classified as pure *P. pinea* stands, 39 as mixed *P. pinea* stands, 19 as pure *Q. pyrenaica* stands and 14 as *P. pinaster* stands.

Table 2. Summary of the mean, range and standard deviation of the main stand variables in the sample plots.

	Pure *Pinus pinea* (*n*=120)				Mixed *Pinus pinea* (*n*=39)			
Variables	Range		Mean	SD	Range		Mean	SD
N (trees ha^{-1})	26.32	1026.32	225.00	152.87	52.60	1605.30	359.65	300.50
G (m^2 ha^{-1})	1.1	28.9	14.0	6.23	0.90	37.60	12.31	8.41
Vcc (m^3 ha^{-1})	4.1	141.9	63.1	32.62	2.40	193.40	57.74	43.42
H_m (m)	3.83	13.34	9.00	2.33	2.07	13.30	7.73	1.81
SH (m)	3.93	13.58	9.30	2.65	2.81	14.49	8.47	2.77
H_0 (m)	4.00	13.83	9.92	2.48	5.30	14.70	10.38	2.49
CBH (m)	0.35	7.33	2.52	1.25	0.70	7.55	2.39	1.42
	Quercus pyrenaica (*n*=19)				*Pinus pinaster* (*n*=14)			
Variables	Range		Mean	SD	Range		Mean	SD
N (trees ha^{-1})	26.32	1368.42	486.15	395.75	52.63	2157.89	1077.07	785.79
G (m^2 ha^{-1})	0.34	19.20	7.57	6.35	1.33	59.37	29.41	91.79
Vcc (m^3 ha^{-1})	1.98	96.42	38.80	31.40	7.58	302.59	152.44	94.97
H_m (m)	5.59	8.84	7.16	1.01	7.03	13.99	9.55	1.61
SH (m)	5.74	8.98	7.19	1.08	8.32	14.59	10.28	1.60
H_0 (m)	5.81	11.17	8.07	1.73	10.83	15.22	11.92	1.13
CBH (m)	0.40	2.60	1.50	1.96	2.80	9.60	3.82	2.46

2.3. LiDAR data

LiDAR data were acquired for the PNOA project, between July and August 2010 and under the direction of the Spanish Ministry of Public Works and Transport (*Dirección General del Instituto Geográfico Nacional, IGN*, and *Centro Nacional de Información Geográfica, CNIG*), using an LEICA ALS50 sensor operated at 1064 nm, a maximum pulse repetition rate of 83 kHz, a maximum scan frequency of 32.1 Hz, a maximum scan angle of ±50° and an average flying height of 2866 m.a.s.l. A maximum of 4 returns per pulse were registered, with a theoretical laser pulse density required for the PNOA project of 0.5 first returns m^{-2}. Summary statistics of first return density per square metre within plots are as follows: average = 1.76, minimum = 1, maximum = 41 and standard deviation = 1.62.

2.4. LiDAR metrics

LiDAR metrics are structural descriptive statistics calculated from the normalised laser-derived point cloud. The metrics for the 192 plots were calculated using the FUSION LiDAR Toolkit (McGaughey, 2014). In summary, LiDAR metrics were computed for each circular plot after normalising the data by subtracting the DEM (Digital Elevation Model). For further details of the procedure used to obtain the LiDAR metrics, see González-Ferreiro *et al.* (2014). The variables related to height distribution and canopy closure were thus obtained. Furthermore, a set of metrics related to the density of returns enclosed in the vertical space defined by five intervals was calculated, after establishing the *MHT* and *HBT*. The LiDAR metrics are summarised and described in Table 3 and Table 4.

Table 3. Potential explanatory LiDAR metrics related to height distribution.

Variables related to height distribution (m)	Description
h_{min}, h_{max}, h_{mean}, h_{mode}, h_{median}	minimum, maximum, mean, mode, median
h_{SD}, $h_{CV,}$ h_{VAR}	standard deviation, coefficient of variation, variance
h_{skw}, h_{kurt}, h_{ID}	skewness, kurtosis, interquartile distance
h_{AAD}	average absolute deviation
$h_{MADmedian}$	median of the absolute deviations from the overall median
$h_{MADmode}$	median of the absolute deviations from the overall mode
h_{L1}, h_{L2}, ..., h_{L4}	L-moments
h_{Lskw}	L-moment of skewness
h_{Lkurt}	L-moment of kurtosis
h_{05}, h_{10}, h_{20}, ..., h_{90}, h_{95}	percentiles

Table 4. Potential explanatory LiDAR metrics related to canopy closure.

Variables related to canopy closure (%)	Description
CRR	[(mean height – min height) / (max height – min height)]
PFRAHBT	Percentage of first returns above *HBT* / Total all returns
PARAHBT	Percentage of all returns above *HBT* / Total all returns
ARAHBT/TFR	(All returns above *HBT*) / (Total first returns) × 100
PFRAM	Percentage first returns above mean / Total all returns
PARAM	Percentage all returns above mean / Total all returns
PFRAMO	Percentage first returns above mode / Total all returns
PARAMO	Percentage all returns above mode / Total all returns
ARAM/TFR	(All returns above mean) / (Total first returns) × 100
ARAMO/TFR	(All returns above mode) / (Total first returns) × 100
$PAR_{S\ 0\text{-}HBT}$, $PAR_{S\ (HBT\text{-}8)*}$, $PAR_{S\ 8\text{-}14}$, $PAR_{S\ 14\text{-}20}$, $PAR_{S\ 20\text{-}26}$	Ratios of the number of all laser hits within the height strata 0-*HBT*, (*HBT*-8)*, 8-14, 14-20, and 20-26 m (respectively) to the number of all laser hits for each plot

**(HBT-8) strata is shifted for (CBH-HBT[#]) in 3 and 4 threshold height combinations (described in Table 5).*

[#]HBT values for the different type of forest (see Table 5).

The *MHT* establishes the lower boundary for computation of height metrics, and the *HBT* represents a reference level for calculation of canopy density metrics. The *MHT* values considered were fixed values of 1 m, 2 m and also the canopy base height (*CBH*) for each forest type, thus defining the limits between laser canopy echoes and below-canopy echoes. The *HBT* values considered were a fixed value of 2 m, the *CBH* for each forest type, and the average middle crown length for each forest type, i.e. $(H_m\text{-}CBH)/2 + CBH$. According to plot analysis, the *CBH* ranged between 1.5 m for *Q. pyrenaica* forests and 3.82 m for *P. pinaster* forests. In the case of *SH* estimation, the *MHT* values tested ranged from the maximum *MHT* for each forest type to zero. Different combinations of each stand variable (*SH*, *G* and *V*) for the different height thresholds (*MHT* and *HBT*) are shown in Table 5.

Table 5. Combination of threshold heights (*MHT* and *HBT*) for each stand variable.

Variables	Combination	*MHT*(m)	*HBT*(m)
G, V	*(1)*	2	2
	(2)	1	2
	(3)	*CBH*	*CBH*
	(4)	*CBH*	[#]$(H_m\text{-}CBH)/2+CBH$
SH	*(1)*	2	2
	(2)	1	2
	(3)	*CBH*	*CBH*
	(4)	*CBH/2*	*CBH*
	(5)	0.25	*CBH*
	(6)	0	*CBH*

[#]HBT =5.76 m (Pure *P. pinea* forest); *HBT* =5.78 m (Mixed *P. pinea* forest); *HBT* =6.68 m (*P. pinaster* forest); *HBT* =4.34 m (*Q. pyrenaica* forest).

2.5. Modelling

The stepwise selection procedure (Næsset 2011, González-Ferreiro *et al.,* 2012) was used to select the best metrics for estimating *SH*, *G* and *V*. The stepwise selection procedure was performed using R software, specifically the leaps package (R Core Team, 2014). Collinearity between regressors was avoided by checking the condition index (CI) and the variance inflation factor (VIF) at the end of each stepwise procedure. Regressions with a CI above 30 or VIF above 10 were disregarded (Belsley *et al.,* 2005) and a maximum 4 explanatories was used. The Linear models were used to establish forest-specific empirical relationships between field measurements and LiDAR variables. The general expression is as follows:

$$Y=\beta_0+\beta_1X_1+\beta_2X_2+\ldots+\beta_nX_n+\varepsilon \quad (1)$$

where Y is represents the different field variables: *SH* (m), V ($m^3\ ha^{-1}$), G ($m^2\ ha^{-1}$) and $X_1, X_2, \ldots, X_n$ are metrics derived from LiDAR dataset. Comparison of the estimates for the selected models was based on the adjusted coefficient of determination (adj. R^2) and the relative Root Mean Square Error (rRMSE).

2.6. Height threshold analysis

The effect of *HT* was studied initially comparing the goodness-of-fit statistics of the final models, following Næsset (2011), and not on the relation of the metrics themselves with the field attribute. In this case, if an automated procedure for metric selection is used, the entry or exit of different

metrics into the model could compensate or mitigate the effects of the changes in *HT*. The REG procedure of SAS/STAT® (SAS Institute Inc., 2004) was used to analyse the effect of threshold heights metric-by-metric for a better understanding of the *HT* on LiDAR metrics computation. Each of the explanatory metrics of the best model (best height threshold, *BHT*) by dependent variable were compared with the same metrics, extracted using the remaining threshold options. For this purpose, an analysis of variance (ANOVA) and Tukey's test for multiple pairwise comparisons were performed to determine whether there were significant differences among the datasets.

2.7. Mapping stand variables

Mapping was performed by applying the best forest type-specific models to LiDAR data. A regular grid that covered the entire study site was first generated; a cell size of 380.13 m^2 was chosen to closely match the spatial unit for which the models were fitted (i.e. over circular study plots of diameter 22 m). The FUSION LiDAR Toolkit (McGaughey, 2014) was then used to obtain values (per cell) for the explanatory variables and to export these to raster files, which were subsequently used in a Geographic Information System (GIS) to obtain improved *SH*, *G* and *V* maps by applying the specific LiDAR models finally selected for each forest type (see the steps described in Guerra-Hernández *et al.* (2015).

Table 6. Summary of stand variable prediction models and assessment of plot-level accuracy for pure and mixed forest of *P. pinea*. *G* (m^2 ha^{-1}): Basal Area; *V* (m^3 ha^{-1}): Volume over bark; Lorey´s mean stand height (*SH)*.

	Threshold	Independent variables[1]	R^2_{adj}	RMSE	rRMSE(%)
Pure *P. pinea* (*n*=120)					
SH	3	h_{70}^{***}, $h_{kurt\ S\ 14\text{-}20}^{***}$	0.77	1.26	13.55
	1	h_{80}^{***}, $h_{mode\ S\ 2\text{-}8}^{*}$	0.75	1.30	13.98
	4	h_{75}^{***}, $h_{kurt\ S\ 14\text{-}20}^{***}$	0.79	1.21	13.01
	2	$\boldsymbol{h_{75}^{***}}$, $\boldsymbol{h_{VAR}^{***}}$, $\boldsymbol{h_{ADD}^{***}}$	**0.80**	**1.18**	**12.68**
	5	h_{90}^{***}, $h_{kurt\ S\ 14\text{-}20}^{***}$	0.78	1.25	13.44
	6	h_{99}^{***}, $h_{mean\ S\ 14\text{-}20}^{***}$	0.70	1.47	15.80
G	1	h_{10}^{***}, *ARAM/TFR****	0.67	3.65	26.25
	2	$\boldsymbol{h_{10}^{***}}$, ***ARAM/TFR******, ***ARAMO/TFR*****	**0.68**	**3.61**	**25.78**
	3	h_{10}^{***}, *ARAMO/TFR****, $h_{mean\ 8\text{-}14}^{***}$	0.53	4.25	30.35
	4	h_{10}^{***}, *ARAMO/TFR****, $h_{mode\ 8\text{-}14}^{***}$	0.54	4.24	30.28
V	1	h_{mean}^{***},*CRR***, *PARA2****	0.74	16.72	26.50
	2	$\boldsymbol{h_{mean}^{***}}$, ***PFRA2******, ***PFRAMO******	**0.74**	**16.65**	**26.38**
	3	h_{L2}^{**}, h_{mean2}^{***}, $h_{min\ S\ 2.5\text{-}5.7}^{*}$, $h_{min\ S\ 5.7\text{-}14}^{*}$	0.61	20.27	32.12
	4	h_{mean}^{***}, *PARAMO****	0.66	19.1	30.26
Mixed Forest (*n*=39)					
SH	3	h_{60}^{***}, *PFRA2.4**, $PAR_{S\ 0\text{-}2}^{*}$	0.56	1.84	21.72
	1	$\boldsymbol{h_{50}^{***}}$, ***PFRA2****, ***PFRAMO****	**0.61**	**1.80**	**20.42**
	4	h_{70}^{***}, *PFRA2.4**, $PAR_{S\ 0\text{-}2}^{*}$	0.53	1.90	22.43
	2	h_{70}^{***}, *PFRA2**, $PAR_{S\ 0\text{-}2}^{*}$	0.53	1.88	22.19
	5	h_{L1}^{***}, *PFRA2.4****, $PAR_{S\ 14\text{-}20}^{*}$	0.54	1.87	22.07
	6	h_{L1}^{***}, *PFRA2.4***, $PAR_{S\ 14\text{-}20}^{*}$	0.48	1.99	23.49
G	**1**	$\boldsymbol{h_{95}^{***}}$, ***PARA2*****, $\boldsymbol{h_{mean\ S\ 2\text{-}8}^{***}}$, $\boldsymbol{h_{mean\ S\ 8\text{-}14}^{**}}$	**0.77**	**4.00**	**32.52**
	2	$h_{mean\ S\ 2\text{-}8}^{***}$, $h_{max\ S\ 14\text{-}20}^{***}$, *PARA2****	0.75	4.18	33.96
	3	$PAR_{S\ 5.7\text{-}14}^{***}$, $h_{skw\ S\ 0\text{-}2}^{***}$, $h_{max\ S\ 14\text{-}20}^{**}$,$h_{mean\ S\ 5.70\text{-}14}^{*}$	0.73	4.37	35.50
	4	h_{20}^{***}, h_{kurt}^{*}, $PAR_{S\ 0\text{-}2.40}^{***}$, $h_{mode\ S\ 0\text{-}2.40}^{*}$	0.67	4.77	38.74
V	1	$h_{mean\ S\ 2\text{-}8}^{***}$, h_{80}^{*}, *PFRAMO**, $h_{max\ S\ 14\text{-}20}^{*}$	0.71	23.38	40.02
	2	h_{90}^{***}, $h_{mode\ S\ 2\text{-}8}^{***}$	0.64	26.23	45.42
	3	$\boldsymbol{PARAM^{***}}$, $\boldsymbol{h_{cv\ S\ 0\text{-}2.40}^{***}}$, $\boldsymbol{h_{skw\ S\ 0\text{-}2.40}^{***}}$, $\boldsymbol{PAR_{S\ 14\text{-}20}^{***}}$	**0.82**	**18.45**	**31.95**
	4	*PARAM****, $h_{cv\ S\ 0\text{-}2.40}^{***}$, $h_{skw\ S\ 0\text{-}2.40}^{***}$, $PAR_{S\ 14\text{-}20}^{***}$	0.82	18.45	31.95

[1] Pr(>|*t*|) *p*=<0.0001 '***' <0.001 '**' <0.01 '*' <0.05.

3. Results

The models selected for each type of forest and each combination of *HT* are shown in Tables 6 and 7. The best models are highlighted in bold type in Tables 6 and 7. Regressions explained 61-85%, 67-98% and 74-98% of the variability in field estimated *SH*, *G* and *V*, respectively. In terms of rRMSE, values ranged from 6.8-20.59%, 7.95-32.62%, and 8.9-31.95%, respectively. The estimates of forest stand parameters in *P. pinea* and pure *P. pinaster* stands were more accurate than those obtained for the mixed forest and *Q. pyrenaica* forest with a more complex vegetation structure.

The canopy threshold did not have a clear effect on the accuracy of *V* and *G* models, although some differences were observed when *MHT* and *HBT* increased to *CBH* and to the average middle crown length in *V* modelling for mixed and deciduous forest, respectively. The best values for *MHT* and *HBT* in *V* modelling varied between the different types of forest, from *MHT* = 1-2 m and *HBT* = 2 m (coniferous stands) to *MHT* = 1.50-2.46 m and *HBT* = 4.34-2.40 m (*Q. pyrenaica* forest and mixed forests, respectively). The best values for *G* modelling ranged from *MHT* = 1-2 m, *HBT* = 2 m (coniferous stands) to *MHT* = 2 m, *HBT* = 2 m (*Q. pyrenaica* forest and mixed forests, respectively). The optimal *MHT* value for SH estimation should be close to 1 m for pure stands and close to 2 m for mixed and *Q. pyrenaica* forests.

The ANOVA and Tukey's test for multiple pairwise comparisons (Table 8) showed that many explanatory variables within the best model (best

Table 7. Summary of stand variable prediction models and results of plot-level accuracy assessment for *P. pinaster* and *Q. pyrenaica*; Density; *G* (m^2 ha^{-1}): Basal Area; *V* (m^3 ha^{-1}):Volume over bark; H_L(m): Lorey´s mean stand height (*SH*).

	Threshold	Independent variables[1]	R^2_{adj}	RMSE	rRMSE(%)
Pure *P. pinaster* (*n*=14)					
SH	3	h_{L4}^{**}, h_{05}^{*}, $h_{mean\ S\ 20\text{-}26}^{***}$	0.80	0.71	6.90
	1	$h_{max\ S\ 0\text{-}2}^{*}$, $h_{mode\ S\ 14\text{-}20}^{**}$, $h_{SD\ S\ 20\text{-}26}^{**}$	0.81	0.69	6.71
	4	h_{L4}^{**}, h_{05}^{*}, $h_{SD\ S\ 20\text{-}26}^{***}$	0.83	0.66	6.42
	2	$\boldsymbol{h_{max\ S\ 0\text{-}2}^{*}}$, $\boldsymbol{h_{max\ S\ 14\text{-}20}^{**}}$, $\boldsymbol{h_{kurt\ S\ 14\text{-}20}^{**}}$	**0.85**	**0.62**	**6.01**
	5	$h_{min\ S\ 0\text{-}2}^{*}$, $h_{median\ S\ 0\text{-}2}^{**}$, $h_{median\ S\ 20\text{-}26}^{**}$	0.79	0.72	7.00
	6	h_{99}^{***}, h_{mean}^{*}, $h_{max\ S\ 6.70\text{-}14}^{**}$	0.73	0.82	7.98
G	**1**	$\boldsymbol{PFRAM^{***}}$, $\boldsymbol{h_{SD\ S\ 0\text{-}2}^{***}}$, $\boldsymbol{h_{kurt\ S\ 2\text{-}8}^{***}}$	**0.98**	**2.34**	**7.95**
	2	$PFRAM^{***}$, $h_{SD\ S\ 0\text{-}2}^{***}$, $h_{kurt\ S\ 2\text{-}8}^{***}$	0.98	2.51	8.53
	3	$PARA3.80^{***}$, h_{mode}^{**}, $h_{median\ S\ 3.80\text{-}6.70}^{**}$	0.93	4.78	16.25
	4	$PARA3.80^{***}$, h_{mode}^{**}, $h_{median\ S\ 3.80\text{-}6.70}^{**}$	0.93	4.78	16.25
V	**1**	$\boldsymbol{PFRAM^{***}}$, $\boldsymbol{PAR_{S\ 2\text{-}8}^{**}}$, $\boldsymbol{h_{kurt\ S\ 2\text{-}8}^{***}}$	**0.98**	**13.65**	**8.9**
	2	$PFRAM^{***}$, $PAR_{S\ 2\text{-}8}^{**}$, $h_{kurt\ S\ 2\text{-}8}^{***}$	0.98	13.77	9
	3	$PARA3.80^{***}$, $h_{kurt\ S\ 0\text{-}3.80}^{**}$, $h_{skw\ S\ 6.70\text{-}14}^{**}$	0.90	29.46	19.32
	4	$ARA6.70/TFR^{***}$, $h_{kurt\ S\ 0\text{-}3.80}^{**}$, $h_{skw\ S\ 6.70\text{-}14}^{**}$	0.91	28	18.01
Q. pyrenaica (*n*=19)					
SH	**1**	$\boldsymbol{h_{20}^{***}}$, $\boldsymbol{h_{60}^{***}}$, $\boldsymbol{h_{max\ S\ 0\text{-}2}^{***}}$, $\boldsymbol{h_{sd\ S\ 0\text{-}2}^{*}}$	**0.84**	**0.45**	**6.25**
	3	h_{05}^{**}, $h_{mode\ S\ 1.50}^{**}$, $h_{max\ S\ 1.5\text{-}4.30}^{*}$	0.65	0.63	8.76
	2	h_{60}^{***}, $h_{min\ S\ 0\text{-}2}^{*}$, $h_{max\ S\ 0\text{-}2}^{***}$, $h_{CV\ S\ 0\text{-}2}^{*}$	0.76	0.53	6.25
	4	h_{mean2}^{***}, $h_{mode\ S\ 0\text{-}1.5}^{***}$, $h_{SD\ S\ 1.5\text{-}4.30}^{**}$, $PAR_{S\ 4.30\text{-}14}^{***}$	0.82	0.46	6.39
	5	$h_{mode\ S\ 0\text{-}1.5}^{**}$, $h_{median\ S\ 1.50\text{-}4.30}^{***}$, $PAR_{S\ 4.30\text{-}14}^{**}$, $h_{mean\ S\ 4.30\text{-}14}^{**}$	0.80	0.48	6.67
	6	$h_{min\ S\ 4.30\text{-}14}^{*}$, $h_{median\ S\ 4.30\text{-}14}^{***}$	0.52	0.74	10.29
G	**1**	$\boldsymbol{h_{10}^{***}}$, $\boldsymbol{h_{25}^{***}}$, $\boldsymbol{PAR_{S\ 2\text{-}8}^{*}}$	**0.86**	**2.47**	**32.62**
	2	h_{10}^{***}, h_{30}^{***}, $PAR_{S\text{-}2\text{-}8}^{*}$	0.81	2.76	36.45
	3	h_{Lskw}^{*}, $h_{skw\ S\ 0\text{-}1.5}^{**}$, $h_{mode\ S\ 1.50\text{-}4.30}^{*}$, $PAR_{S\ 4.30\text{-}14}^{***}$	0.83	2.58	34.08
	4	$ARA4.30/TFR^{***}$, $h_{skw\ S\ 0\text{-}1.5}^{**}$, $h_{mode\ S\ 1.50\text{-}4.30}^{*}$	0.83	2.62	34.61
V	1	h_{60}^{***}, $PARAMO^{***}$, $ARAM/TFR^{***}$, $PAR_{S\ 0\text{-}2}$	0.85	12.25	31.57
	2	h_{90}^{***}, $h_{MADmode}^{**}$, $h_{max\ S\ 0\text{-}2}^{**}$, $h_{mean\ S\ 2\text{-}8}^{***}$	0.81	14.07	36.26
	3	h_{skw}^{***}, $PFRA1.50^{***}$, $h_{kurt\ S\ 0\text{-}1.50}^{***}$, $h_{mode\ S\ 1.50\text{-}4.30}^{*}$	0.82	13.43	34.61
	4	$\boldsymbol{PFRA4.30^{***}}$, $\boldsymbol{h_{max\ S\ 0\text{-}1.50}^{**}}$, $\boldsymbol{h_{SD\ S\ 0\text{-}1.50}^{***}}$, $\boldsymbol{h_{mode\ S\ 1.50\text{-}4.30}^{***}}$	**0.88**	**10.95**	**28.22**

[1] Pr(>|*t*|) *p*=<0.0001 '***' <0.001 '**' <0.01 '*' <0.05.

height threshold *BHT*) by dependent variable, were statistically different compared with the same metrics from the remaining thresholds combinations. Intermediate *(h_{mean}, h_{60})* and upper height percentiles (h_{95}), influenced by the *MBT*, have suffered fewer the effect of *HT* changes than lower height metrics (h_{10}) (see Table 8). Density metrics that depend on fixed value of *HBT* (*PFRA2*, *PARA2*, and *PFRA4.30*) showed greater differences, maybe because *HBT* presents a wider range of variation. In most of the cases, the metric-by-metric threshold analysis showed significant differences, although is difficult to identify clear tendencies, due to the large variety of metrics, thresholds, forest types and dependent variables combinations analyzed in this study. Even so, threshold options 5 and 6 seem to be high different from the best selected threshold for *SH* in most of forest types and very different combinations, like 1 and 2 respect to 3 and 4 also show significant differences in the metric-by-metric analysis.

Figure 2 shows LIDAR-based stand variable predictions in comparison with the stand-based forest variable estimates in the sample plots of each forest type.

Table 8. Metric-by-metric height threshold analysis: All selected explanatory variables for the best models (best height threshold, *BHT*) by dependent variable and forest type were compared with the same metrics obtained from the remaining height thresholds. Only the lowest *p-values* for the Tukey's test for pairwise comparison are showed in the table. The numbers in brackets below *p-values* refer to the option of height threshold corresponding to the lowest found *p-value* (*HT*).

			ANOVA (Tukey test)			
	BHT	Independent variables	*p-value* (*HT*)			
		Pure *P. pinea* (*n*=120)	a	b	c	
SH	2	***a) h_{75}, b) h_{VAR}, c) h_{ADD}***	**<0.05 (6)**	**<0.05 (6)**	**<0.05 (6)**	
G	2	***a) h_{10}, b) ARAM/TFR, c) ARAMO/TFR***	**<0.05 (3,4)**	0.19 (4)	0.69 (3)	
V	2	***a)h_{mean}, b)PFRA2, c) PFRAMO***	0.6548 (3,4)	**<0.05 (4)**	**<0.05 (3,4)**	
		Pure *P. pinaster* (*n*=14)				
SH	2	***a) $h_{max\ S\ 0\text{-}2}$, b) $h_{max\ S\ 14\text{-}20}$, c) $h_{Kurt\ S\ 14\text{-}20}$***	**<0.05 (3,4,5,6)**	**1**	**1**	
G	1	***a)PFRAM, b) $h_{SD\ S\ 0\text{-}2}$, c) $h_{kurt\ S\ 2\text{-}8}$***	0.51 (3,4)	**<0.05 (3,4)**	0.74 (3,4)	
V	1	***a) PFRAM, b) PAR $_{S\ 2\text{-}8}$, c) $h_{kurt\ S\ 2\text{-}8}$***	0.5 (3,4)	0.13 (3,4)	0.74 (3,4)	

			ANOVA (Tukey test)			
	BHT	Independent variables	*p-value* (*HT*)			
		Mixed Forest (*n*=39)	a	b	c	d
SH	1	***a) h_{50}, b) PFRA2, c) PFRAMO***	**<0.05 (6)**	**<0.05 (3,4,5,6)**	**<0.05 (5,6)**	
G	1	***a) h_{95}, b) PARA2, c) $h_{mean\ S\ 2\text{–}8}$, $h_{mean\ S\ 8\text{-}14}$***	0.96 (3,4)	**<0.05 (4)**	**<0.05 (3,4)**	**<0.05 (3,4)**
V	3	***a) PARAM, b) $h_{cv\ S\ 0\text{-}2.40}$, c) $h_{skw\ S\ 0\text{-}2.40}$, d) PAR $_{S\ 14\text{-}20}$***	0.29 (1)	0.96 (1,2)	0.98 (1,2)	**1**
		Q. pyrenaica (*n*=19)				
SH	1	***a) h_{20}, b) h_{60}, c) $h_{max\ S\ 0\text{-}2}$, d) $h_{sd\ S\ 0\text{-}2}$***	**<0.05** (2,3,4,5,6)	0.96 (6)	**<0.05 (5,6)**	**<0.05 (5,6)**
G	1	***a) $h_{10,}$ b) h_{25}, c) PAR $_{S\ 2\text{-}8}$***	0.20 (2)	0.83 (2)	0.70 (3,4)	
V	4	***a) PFRA4.30, b) $h_{max\ S\ 0\text{-}1.50}$, c) $h_{SD\ S\ 0\text{-}1.50}$, d) $h_{mode\ S\ 1.50\text{-}4.30}$***	0.08 (3)	**<0.05 (1,2)**	**<0.05 (1,2)**	**<0.05 (1,2)**

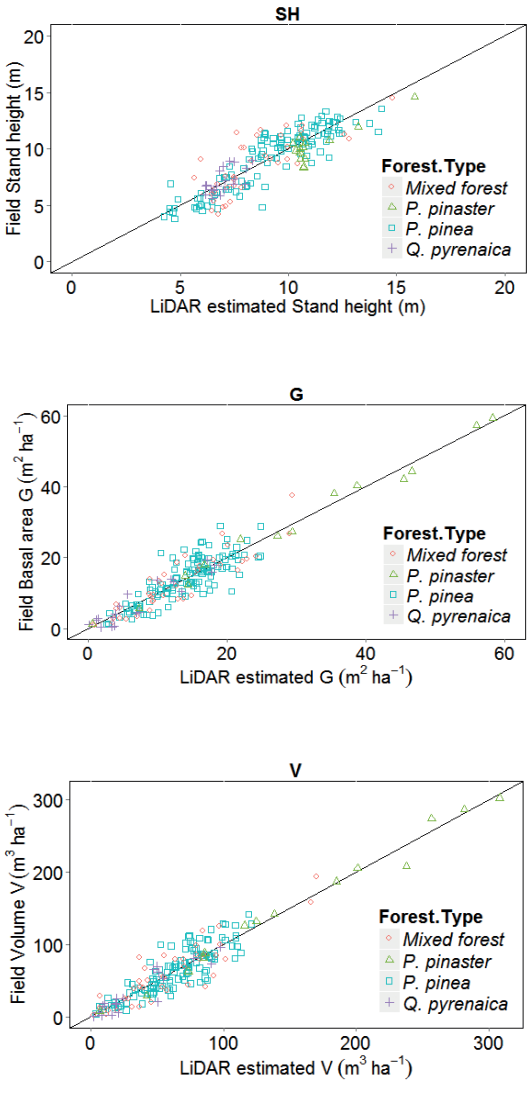

Figure 2. Scatterplots and 1:1 line for the field-measured and the best model-estimated results for the sample plots.

Finally, spatially-explicit maps obtained by applying the best forest-specific models to the LiDAR data, which provides a single value per cell for the target stand variable (*SH*, *G* and *V*), are shown in Figure 3.

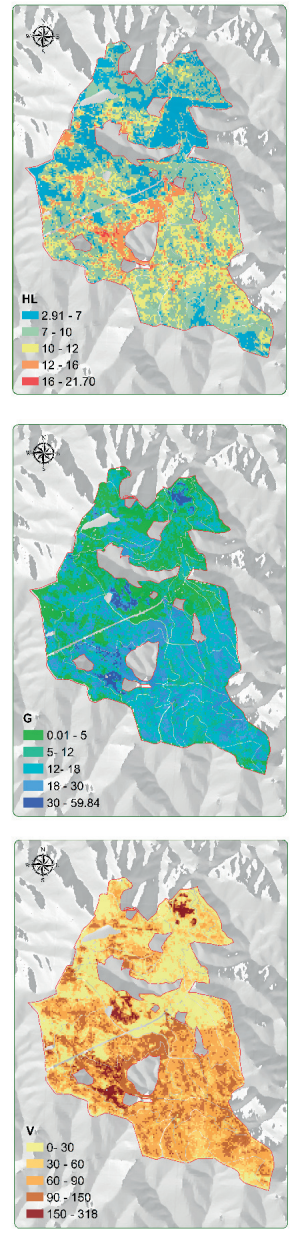

Figure 3. Maps of biometric variables across the research site (pixel size = 22 m).

4. Discussion and conclusions

Mapping has always been essential in forest inventories, fire management planning and biomass exploitation in order to obtain spatially explicit geographic information about forest stocks and their distribution. In the Mediterranean basin, these tasks are particularly challenging because of the extremely high degree of variability in composition, volume, quality and orography of the forests. Forest inventories can be used to provide

estimates of natural resources at national, regional and local scales, to meet reporting requirements and to support policy and management decision making processes. Unfortunately, field data acquisition from wide areas is generally time consuming and expensive (Hall *et al.,* 2005). The combination of field and LiDAR data has proven a cost-viable alternative for providing accurate estimates (Means *et al.,* 2000).

Airborne LiDAR and multiple-platform laser studies for assessing biophysical parameters in many types of forest ecosystems report reliable results with acceptable uncertainty estimates (Van Leeuwen and Nieuwenhuis, 2010). Laser pulse density and vegetation structure are the most important factors in relation to the height accuracy of the laser-derived Digital Elevation Model (DEM) (Raber *et al.,* 2002; Clark *et al.,* 2004; Valbuena, 2011), especially on steep terrain (Estornell *et al.,* 2011). Furthermore, plot size is an important design parameter in forest surveys, because it has the potential to reduce or inflate the impact of the edge effects and co-registration error, thus affecting the estimated values of forest stand parameters (Ruiz *et al*., 2014). The accuracy of the results (among other factors) also depends on field measurements and allometric equations used to model variables. In this respect, the distribution of LiDAR data points used in the study demonstrated the potential use of very low density LiDAR data and traditional inventory plot sizes for estimating biophysical parameters, even in closed canopy forests with complex vegetation structure (*Q. pyrenaica* stands and mixed forest) and topographically complex terrain (more than 50% of the area with strong slopes ranging between 25-50%).

The results obtained for modelling *SH* in pure coniferous stands (adj. $R^2 = 0.80$-0.85, rRMSE = 2.68%-6.8%) were slightly better in terms of rRMSE than the values obtained for *Pinus sylvestris* and *Picea abies* in Norway (Järnstedt *et al.,* 2012), with a pulse density of 10.43 pulses m^{-2}. However, they were slightly poorer than those reported for *P. radiata* (González-Ferreiro *et al.,* 2014) and for *P. nigra* and *P. pinaster* (González-Olabarria *et al.,* 2012) in Spain, with laser pulse densities of 0.5 and 2 pulses m^{-2}, respectively. In the case of mixed forest (adj $R^2 = 0.61$, rRMSE = 20.42%), the results were similar to those obtained for mixed forest in Italy (adj. $R^2 = 0.64$) (Alberti *et al.*, 2013), with a laser pulse density of 2.8 pulses m^{-2}, and for subtropical rainforest (adj. $R^2 = 0.61$) in complex terrain in Australia (Ediriweera *et al.,* 2014), with a point density of 1-1.3 pulses m^{-2}.

In addition to laser pulse density and the presence of steep areas, other factors may cause errors in predictive LiDAR models. In the present study *i*) the heights of the remaining trees of the plot were estimated, rather than being measured in the field; *ii*) accurate measurement of tree heights was difficult, as broadleaved trees usually have multiple apexes and the highest apex is not systematically located above the trunk, and in the case of *P. pinea*, the crown is rounded or umbrella-shaped because the trees do not display strong apical dominance; and *iii*) as demonstrated in previous studies (Raber *et al.,* 2002; Clark *et al.,* 2004; Estornell *et al.,* 2011) for relatively dense and structural deciduous forest on steep slopes, data characteristics such as scan angle often cause DEM inaccuracies that affect LiDAR-derived canopy height.

Stand basal area estimates derived from linear models for pure stone pine stands (adj. $R^2 = 0.67$, rRMSE = 26.25%) were similar to the values obtained for *Pseudotsuga menziesii* by Coops *et al.* (2007) ($R^2 = 0.65$, plot size=400 m^2) and for *P. radiata* by Stephens *et al.* (2007) ($R^2 = 0.66$, rRMSE = 22.47%, plot size = 200-2450 m^2 and González-Ferreiro *et al.* (2012) ($R^2 = 0.68$, plot size = 225 m^2), but were slightly lower than some estimates for boreal areas (Næsset, 2002) ($R^2 = 0.86$, plot size = 200 m^2) and for forest in Canada (Treitz *et al.,* 2010) ($R^2 = 0.91$-0.94, plot size = 400 m^2). The best values for mixed forest (adj. $R^2 = 0.77$ and rRMSE = 32.52%) were better in terms of adj. R^2 reported for subtropical rainforest (adj. $R^2 = 0.61$, plot size = 2500 m^2), but slightly worse in terms of rRMSE reported for mixed stands in Sweden (21.5-23.2%, plot size = 452.39 m^2) (Lindberg and Hollaus, 2012).

The results of volume modelling for pure *P. pinea* stands (adj. $R^2 = 0.74$, rRMSE = 26.38%) are similar to those reported by González-Ferreiro *et al.* (2012) ($R^2 = 0.69$, rRMSE = 25%), but slightly lower than those reported by Treitz *et al.* (2010) ($R^2 = 0.83$-0.97, rRMSE = 16-22%). For mixed forest, the present results ($R^2 = 0.82$, rRMSE = 31.95 %) are better than those reported for mixed forest ($R^2 = 0.65$, rRMSE = 37.3-41.9%)

in Sweden, with a pulse density of 7 returns m^2 (Lindberg and Hollaus, 2012), and mixed forest in Italy ($R^2 = 0.58$) (Alberti *et al.,* 2013). The results of the present study (in terms of adj. R^2) show that the quality of the models for volume and basal area may be affected by plot size and LiDAR data density. Optimum cost-effective plot size has been shown to be near 500-600 m^2 for this type of forest (Ruiz *et al.,* 2014).

On the other hand, *G* and *V* models utilizing height strata metrics performed better than models from previous studies (Guerra-Hernández *et al.,* 2015), except for more homogeneous pure stone pine stands. However, it is important to note that models including height strata metrics always required more predictor variables than models using metrics without strata, in part due to the compartmentalized nature of this metrics.

We concluded that two of the *HT* values considered yielded models that performed equally well in estimating *G* and *V*, suggesting that an increase of 2 m in the *MHT* may lead to loss of useful information for estimating *G* and *V* in mature homogeneous coniferous stands with little or no understory, whilst a very low value of 1 m in dense and closed structural mixed and deciduous forests may include noise in the canopy data set, as reported by Næsset (2011), probably due to LiDAR metrics that account for the presence of understory and small trees (not used in *G* and *V* calculations). As in other studies in young forest (Næsset, 2011; Gorgens, 2015), the results indicate that a higher value of *HBT* and *MHT* may return better metrics for volume modelling in closed structure deciduous and mixed forests. However, the effect on *G* was not as evident. Although a decrease in the *MHT* value to 1 m improved the models for *SH* in coniferous stands, the optimal value was close to 2 m in dense and closed structural mixed and deciduous forests. The optimal solution for each forest type would be to consider a compromise between eliminating noise without loss of any explanatory power, depending on the type of forest and the study variables.

The datasets of the threshold combinations were not completely independent at the beginning of each stepwise procedure, however, the results showed there were many significant differences among the metrics from the best model (specially the dataset combinations 1 and 2 respect to 3 and 4), as revealed by ANOVA analysis. We can conclude that it is not simply a question of replacement but rather that independent variables truly change when *HBT* and *MHT* are modified. The study of the effect of threshold heights metric-by-metric suggested such research would undergo with a high density dataset, since the low density nature of the dataset would also make these threshold heights to have a lesser effect.

In conclusion, this study demonstrated that low-density LiDAR data can be used to obtain important forest stand variables in closed deciduous, mixed forest and open canopy *P. pinea*-dominated forest, in topographically complex terrain. Most of the estimates in open canopy stone pine-dominated forest were accurate and similar to those obtained in related studies. Despite the structural complexity of the mixed and deciduous forest and the steep terrain, it was possible to obtain estimates of structural parameters with a satisfactory level of accuracy. The results confirm that the accuracy of LiDAR estimates of vegetation structure depends on the complexity of the horizontal and vertical structural diversity of the vegetation (Estornell *et al.,* 2011; Valbuena *et al.,* 2011). The study also demonstrates the importance of separating the returns from the canopy and from below canopy and of considering biological aspects during definition of *HT*.

Finally, forest technicians and scientists should work together to standardize the new terminology used in mapping and the parameters established from LiDAR data and also to discuss the best use of LiDAR technology. As LiDAR costs continue to decline and new and easier methods of processing data are developed, managers may incorporate LiDAR data in forest management, particularly where spatially-detailed information on forest structure is required across large spatial scales. However, to date little effort has been made to develop protocols for data acquisition and processing, representing a move towards cost-effective implementation of the technology and reduce the cost of forest inventories, which would be beneficial to governments, landowners and the forest industry.

Acknowledgements

Thanks to: *i*) the Portuguese Science Foundation (SFRH/BD/52408/2013); *ii*) the Galician Government and European Social Fund (Official Journal of Galicia – DOG nº 52, 17/03/2014 p. 11343, exp: POS-A/2013/049); *iii*) the foresters of the Extremadura Forest Service *iv*) Dr. Juan Gabriel Álvarez González (Department of Agroforestry Engineering, University of Santiago de Compostela) for the relevant remarks, suggestions and his advice using the statistical software SAS/STAT; and *v)* anonymous referees of "Revista de Teledetección", whose comments helped us to improve the article.

The research was carried out in the Centro de Estudos Florestais: a research unit funded by Fundação para a Ciência e a Tecnologia (Portugal) within UID/AGR/00239/2013.

References

Alberti, G., Boscutti, F., Pirotti, F., Bertacco, C., De Simon, G., Sigura, M., Cazorzi, F., Bonfanti, P. 2013. A LiDAR-based approach for a multi-purpose characterization of Alpine forests: an Italian case study. *iForest-Biogeosciences and Forestry,* 6(3), 156.

Andersen, H.E., McGaughey, R.J., Reutebuch, S.E. 2005. Estimating forest canopy fuel parameters using LIDAR data. *Remote sensing of Environment*, 94(4), 441-449. http://dx.doi.org/10.1016/j.rse.2004.10.013

Belsley, D.A., Kuh, E., Welsch, R.E. 2005. *Regression diagnostics: Identifying influential data and sources of collinearity*. New Jersey: John Wiley & Sons.

Clark, M.L., Clark, D.B., Roberts, D.A. 2004. Small-footprint lidar estimation of sub-canopy elevation and tree height in a tropical rain forest landscape. *Remote Sensing of Environment*, 91(1), 68-89. http://dx.doi.org/10.1016/j.rse.2004.02.008

Coops, N.C., Hilker, T., Wulder, M.A., St-Onge, B., Newnham, G., Siggins, A., Trofymow, J. T. 2007. Estimating canopy structure of Douglas-fir forest stands from discrete-return LiDAR. *Trees*, 21(3), 295-310. http://dx.doi.org/10.1007/s00468-006-0119-6

Ediriweera, S., Pathirana, S., Danaher, T., Nichols, D. 2014. LiDAR remote sensing of structural properties of subtropical rainforest and eucalypt forest in complex terrain in North-eastern Australia. *Journal of Tropical Forest Science*, 26(3), 397-408.

Estornell, J., Ruiz, L.A., Velázquez-Martí, B., Hermosilla, T. 2011. Analysis of the factors affecting LiDAR DTM accuracy in a steep shrub area. *International Journal of Digital Earth*, 4(6), 521-538. http://dx.doi.org/10.1080/17538947.2010.533201

García, M., Riaño, D., Chuvieco, E., Danson, F.M. 2010. Estimating biomass carbon stocks for a Mediterranean forest in central Spain using LiDAR height and intensity data. *Remote Sensing of Environment*, 114(4), 816-830. http://dx.doi.org/10.1016/j.rse.2009.11.021

Gonçalves-Seco, L., González-Ferreiro, E., Diéguez-Aranda, U., Fraga-Bugallo, B., Crecente, R., Miranda, D. 2011. Assessing the attributes of high-density *Eucalyptus globulus* stands using airborne laser scanner data. *International Journal of Remote Sensing*, 32(24), 9821-9841. http://dx.doi.org/10.1080/01431161.2011.593583

González-Ferreiro, E., Diéguez-Aranda, U., Barreiro-Fernández, L., Buján, S., Barbosa, M., Suárez, J.C., Bye, I.J., Miranda, D. 2013. A mixed pixel- and region-based approach for using airborne laser scanning data for individual tree crown delineation in *Pinus radiata* D. Don plantations. *International Journal of Remote Sensing*, 34(21), 7671-7690. http://dx.doi.org/10.1080/01431161.2013.823523

González-Ferreiro, E., Diéguez-Aranda, U., Crecente-Campo, F., Barreiro-Fernández, L., Miranda, D., Castedo-Dorado, F. 2014. Modelling canopy fuel variables for *Pinus radiata* D. Don in NW Spain with low-density LiDAR data. *International journal of wildland fire*, 23(3), 350-362. http://dx.doi.org/10.1071/WF13054

González-Ferreiro, E., Diéguez-Aranda, U., Miranda, D. 2012. Estimation of stand variables in *Pinus radiata* D. Don plantations using different LiDAR pulse densities. *Forestry*, 85(2), 281-292. http://dx.doi.org/10.1093/forestry/cps002

González-Olabarria, J.-R., Rodríguez, F., Fernández-Landa, A., Mola-Yudego, B. 2012. Mapping fire risk in the Model Forest of Urbión (Spain) based on airborne LiDAR measurements. *Forest Ecology and Management*, 282, 149-156. http://dx.doi.org/10.1016/j.foreco.2012.06.056

Görgens, E.B. 2015. LiDAR technology applied to vegetation quantification and qualification. Doctoral Thesis. Universidade de São Paulo.

Guerra-Hernández, J., González-Ferreiro, E., Jurado-Varela, A., Tomé, M. 2015. Uso de LiDAR aerotransportado para la estimación de variables forestales de un bosque Mediterráneo en el suroeste de España (Extremadura). In: *Teledetección: Humedales y Espacios Protegidos. XVI Congreso de la Asociación Española de Teledetección*. Sevilla, Spain, 21-23 October. pp 379-382.

Hall, S.A., Burke, I.C., Box, D.O., Kaufmann, M.R., Stoker, J.M. 2005. Estimating stand structure using discrete-return lidar: an example from low density, fire prone ponderosa pine forests. *Forest Ecology and Management*, 208(1), 189-209. http://dx.doi.org/10.1016/j.foreco.2004.12.001

Järnstedt, J., Pekkarinen, A., Tuominen, S., Ginzler, C., Holopainen, M., Viitala, R. 2012. Forest variable estimation using a high-resolution digital surface model. ISPRS *Journal of Photogrammetry and Remote Sensing*, 74, 78-84. http://dx.doi.org/10.1016/j.isprsjprs.2012.08.006

Jensen, J.L.R., Humes, K.S., Conner, T., Williams, C.J., DeGroot, J. 2006. Estimation of biophysical characteristics for highly variable mixed-conifer stands using small-footprint lidar. *Canadian Journal of Forest Research*, 36(5), 1129-1138. http://dx.doi.org/10.1139/x06-007

Lindberg, E., Hollaus, M. 2012. Comparison of methods for estimation of stem volume, stem number and basal area from airborne laser scanning data in a hemi-boreal forest. *Remote Sensing,* 4(4), 1004-1023. http://dx.doi.org/10.3390/rs4041004

Maltamo, M., Næsset, E., Vauhkonen, J. 2014. *Forestry applications of airborne laser scanning*. Dordrecht: Springer. http://dx.doi.org/10.1007/978-94-017-8663-8

McGaughey, R. 2014. FUSION/LDV: software for LIDAR Data Analysis and Visualization. In: US Department of Agriculture, F.S., Pacific Northwest Research Station, Seattle, USA. 123 pp. (Ed.).

Means, J., Acker S., Fitt, B., Renslow, M., Emerson, L., Hendrix, C. 2000. Predicting forest stand characteristics with airborne scanning LiDAR. *Photogrammetric Engineering and Remote Sensing,* 66(11), 1367-1371.

Montaghi, A., Corona, P., Dalponte, M., Gianelle, D., Chirici, G., Olsson, H. 2013. Airborne laser scanning of forest resources: an overview of research in Italy as a commentary case study. *International Journal of Applied Earth Observation and Geoinformation*, 23(1), 288-300. http://dx.doi.org/10.1016/j.jag.2012.10.002

Montagnoli, A., Fusco, S., Terzaghi, M., Kirschbaum, A., Pflugmacher, D., Cohen, W. B., Chiatante, D. 2015. Estimating forest aboveground biomass by low density lidar data in mixed broad-leaved forests in the Italian Pre-Alps. *Forest Ecosystems*, 2(1), 1-9. http://dx.doi.org/10.1186/s40663-015-0035-6

Nakai, T., Sumida, A., Kodama, Y., Hara, T., Ohta, T. 2010. A comparison between various definitions of forest stand height and aerodynamic canopy height. *Agricultural and forest meteorology*, 150(9), 1225-1233. http://dx.doi.org/10.1016/j.agrformet.2010.05.005

Næsset, E. 2002. Predicting forest stand characteristics with airborne scanning laser using a practical two-stage procedure and field data. *Remote Sensing of Environment*, 80(1), 88-99. http://dx.doi.org/10.1016/S0034-4257(01)00290-5

Næsset, E., Gobakken, T. 2008. Estimation of above- and below-ground biomass across regions of the boreal forest zone using airborne laser. *Remote Sensing of Environment*, 112(6), 3079-3090. http://dx.doi.org/10.1016/j.rse.2008.03.004

Næsset, E., 2011. Estimating above-ground biomass in young forests with airborne laser scanning. *International Journal of Remote Sensing*, 32(2), 473-501. http://dx.doi.org/10.1080/01431160903474970

Nyström, M., Holmgren, J., Olsson, H. 2012. Prediction of tree biomass in the forest–tundra ecotone using airborne laser scanning. *Remote Sensing of Environment*, 123, 271-279. http://dx.doi.org/10.1016/j.rse.2012.03.008

Raber, G.T., Jensen, J.R., Schill, S.R., Schuckman, K. 2002. Creation of digital terrain models using an adaptive lidar vegetation point removal process. *Photogrammetric engineering and remote sensing*, 68(12), 1307-1314.

R Core Team. 2014. R: A language and environment for statistical computing. Vienna: R Foundation for Statistical Computing.

Ruiz, L.A., Hermosilla, T., Mauro, F., Godino, M. 2014. Analysis of the Influence of Plot Size and LiDAR Density on Forest Structure Attribute Estimates. *Forests*, 5(5), 936-951. http://dx.doi.org/10.3390/f5050936

SAS Institute Inc. 2004. SAS/STAT® 9.1 User's Guide. SAS Institute Inc, Cary, NC.

Stephens, P.R., Watt, P.J., Loubser, D., Haywood, A., Kimberley, M.O. 2007. Estimation of carbon stocks in New Zealand planted forests using airborne scanning LiDAR. In: *Proceedings ISPRS Workshop on Laser Scanning 2007 and SilviLaser 2007*, Espoo, Finland, 12-14 September, pp. 389-394.

Treitz, P., Lim, K., Woods, M., Pitt, D., Nesbitt, D., Etheridge, D. 2012. LiDAR Sampling Density for Forest Resource Inventories in Ontario, Canada. *Remote Sensing*, 4(4), 830-848. http://dx.doi.org/10.3390/rs4040830

Valbuena, R., Mauro, F., Arjonilla, F.J., Manzanera, J.A. 2011. Comparing airborne laser scanning-imagery fusion methods based on geometric accuracy in forested areas. *Remote Sensing of Environment*, 115(8), 1942-1954. http://dx.doi.org/10.1016/j.rse.2011.03.017

Van Leeuwen, M., Nieuwenhuis, M. 2010. Retrieval of forest structural parameters using LiDAR remote sensing. *European Journal of Forest Research*, 129(4), 749-770. http://dx.doi.org/10.1007/s10342-010-0381-4